



## Supplementary Material for

### **Sleep Drives Metabolite Clearance from the Adult Brain**

Lulu Xie, Hongyi Kang, Qiwu Xu, Michael J. Chen, Yonghong Liao,  
Meenakshisundaram Thiyagarajan, John O'Donnell, Daniel J. Christensen, Charles  
Nicholson, Jeffrey J. Iliff, Takahiro Takano, Rashid Deane, Maiken Nedergaard\*

\*Corresponding author. E-mail: nedergaard@urmc.rochester.edu

Published 18 October 2013, *Science* **342**, 373 (2013)  
DOI: 10.1126/science.1241224

**This PDF file includes:**

Materials and Methods

Figs. S1 to S5

References

## **Sleep Drives Metabolite Clearance from the Adult Brain**

**Xie et al., Manuscript 1241224**

### **Supplementary Materials and Methods**

All experimental data were collected in male C57/BL6 mice (Charles River, 10-12 weeks). The experiments were approved by the Institution of Animal Care and Use Committee of University of Rochester and efforts were taken to minimize the number of animals used.

#### **2-photon imaging of CSF tracer influx**

For in vivo imaging, mice were anesthetized with 2% isoflurane and a head plate was glued to the skull. The mice were habituated to the microscope stage over the next 2 days during 3-4 training sessions each lasting 30-60 min. At day 3, the animals were again anesthetized with 2% isoflurane and a cranial window was prepared over the right hemisphere at 2.5 mm lateral and 2 mm posterior to bregma. Dura was left intact and the craniotomy (~3 mm diameter) was filled with aCSF and covered with a modified glass coverslip, then sealed with dental cement. A small burr hole was prepared for ECoG recordings over the left hemisphere mirroring the position of the cranial window (2.5 mm lateral and 2 mm posterior to bregma). A 30GA needle was implanted into the cisterna magna and glued to the skull with dental cement. The open end of the needle was inserted into a piece of polyethylene tubing, which was sealed by cauterization. Custom-made EMG leads were inserted in the neck muscle and secured with sutures. All animals were allowed to recover for 4-6 hrs prior to imaging.

To compare arousal state transitions, CSF tracer influx was imaged in 3 different groups: (1) animals that were initially asleep and subsequently woken up by gentle movement of their tails. These imaging data were collected when mice were naturally asleep (12-2 pm). (2) Awake mice that were anesthetized with a mixture of 100 mg/kg ketamine and 10 mg/kg xylazine i.p. These experiments were performed when the mice were naturally awake (8-10 pm). (3) Awake mice in which a mixture of norepinephrine receptor antagonists was administered via the cisterna magna cannula. These experiments were performed at 8-10 pm. The state of brain activity was monitored by ECoG in the contralateral hemisphere and by an EMG electrode

inserted into the neck muscle. The tails of the mice were gently handled during the awake state in all three groups to prevent spontaneous sleep.

To establish the effect of the arousal state on CSF influx, Texas red or FITC labeled dextran with identical molecular weight (3kD, constituted in aCSF at a concentration of 0.5%) were infused up to a total volume of 5  $\mu$ l at a rate of 1 $\mu$ l/min over 5 minutes with a syringe pump. CSF tracer was administered via cisterna magna using a two-way divider fitted to the polyethylene tubing. To visualize the vasculature, the BBB impermeable cascade blue-dextran (MW 10 kD, 1% in saline,) was injected i.v. via the femoral vein. A Ti:Sapphire laser, FV300 laser-scanning system controlled by Fluoview software and an upright microscope were used for *in vivo* imaging as described previously (1). A 20X water immersion lens was used to image tracer influx and the cerebral vasculature. FITC and Texas Red were excited using 820 nm, whereas 800 nm excitation was used for cascade Blue. Red (590-650nm), green (500-550nm), and blue (403-427nm) bandpass filters were used to collect emission fluorescence from Texas Red, FITC, and cascade Blue, respectively. The experiments were designed such that CSF tracer influx could be quantified in two different stages of brain activity in the same mouse: 1) cortical influx of the CSF tracer (alternating FITC- or Texas Red-dextran) was imaged for a total of 30 min, followed by 2) a transition to a different state of brain activity (e.g., sleep to awake; awake to anesthesia; or awake followed by administration of norepinephrine receptor antagonists). The second CSF tracer was infused 15 minutes later and CSF influx imaged for another 30 min. Cortex was repeatedly scanned from the surface to 200  $\mu$ m below the surface at 1 min intervals using 5  $\mu$ m z-steps and 512 x 512 pixel resolution during the 30 min imaging session. ImageJ software with the UCSD plugin set was used for data analysis. Optical sections located 100  $\mu$ m below the cortical surface were selected for the analysis of the kinetics of CSF tracer influx. To define tracer coverage (glymphatic influx), the area ( $\mu$ m<sup>2</sup>) of the optical section with a pixel intensity > 40 (out of 255) was quantified. This area was expressed as the percentage of total area of the optical section. To define perivascular tracer movement, circular regions of interest (ROI) 25 pixels in diameter were defined surrounding penetrating arteriole. To define the exchange of perivascular CSF tracer with interstitial fluid (ISF) of the surrounding parenchyma, donut-shaped ROIs were defined that had an external diameter of 150 pixels and an internal

diameter of 50 pixels. Respectively, these ROIs corresponded to the approximate dimensions of the arteriole plus perivascular regions and a small arbitrary portion of the adjacent parenchyma tissue, thus allowing the exclusion of the perivascular tracer from quantification of pixel intensity, to gain a measure of exchange. The ROIs were centered upon penetrating arterioles. Mean pixel intensity within these ROIs was measured at each time point. When tracer movement along penetrating arterioles, or into peri-arterial brain tissue was compared, a 2-way ANOVA was used followed by Bonferroni's post-hoc test. A 2-way ANOVA was used to compare the differences followed by Bonferroni's post-hoc test. Penetrating arterioles were distinguished from penetrating venules on the basis of the direction of flow as well as morphology: surface arteries are positioned superficially to surface veins and exhibit less branching at superficial cortical depths. For 3D visualization, cascade blue-labeled vasculature was imaged with higher resolution of  $0.7 \times 0.7 \times 0.7 \mu\text{m}$  voxel size. The vasculature was traced and reconstructed using NeuroLucida software. Images of CSF tracers captured at 15 min after cisterna magna administration of the tracers were reconstructed in 3D with NeuroLucida and color-coded before merging the the 3D reconstruction of the vasculature.

The mixture of norepinephrine receptor antagonists (prazosin, atipamezole and propranolol, all at 2 mM) (2) was injected into cisterna magna starting with a bolus of  $5 \mu\text{l}$  at a rate of  $1 \mu\text{l}/\text{min}$  followed by a slower infusion rate of  $0.167 \mu\text{l}/\text{min}$  with a syringe pump until the end of experiment.

### **EEG, ECoG, and EMG recordings and analysis**

Cortical EEG (ECoG) was recorded by insertion of a single barrel electrode (tip diameter of 2-3  $\mu\text{m}$ ) 2.5 mm lateral and 2 mm posterior to bregma to a depth of 150  $\mu\text{m}$  in the contralateral hemisphere to the window prepared for 2-photon imaging to avoid penetrating the ipsilateral dura, which can alter CSF tracer fluxes (3). ECoG and EMG activity were co-currently recorded and compared in awake, sleeping, and anesthetized animals (**Fig. S1**). In all experiments measuring the interstitial space, ECoG was recorded by the reference barrel of the TMA microelectrode. In either case the signals were collected with Clampex 10.2 and broken down into artifact-free 5 min epochs, These epochs were further broken down into the % prevalence

of Delta (0 – 4 Hz), Theta (4 – 7 Hz), Alpha (8 – 13 Hz), and Beta (13 – 20 Hz) power bands as previously described (4-6). Wakefulness was defined as desynchronized low-amplitude ECoG, while sleep states were defined as synchronized high amplitude activity dominated by low frequency waves (0-4 Hz) in artifact-free five minute epochs.

To assess whether the microelectrode recordings of ECoG were representative of standard EEG recordings, we compared ECoG to EEG recordings obtained by commercial telemetric electrodes. The headplate was mounted under 2% isoflurane anesthesia, and small burr holes were drilled in the skull 2.5 mm lateral and 2 mm posterior to bregma on either side of the midline. EEG wire leads were then inserted into the burr holes on one side of the midline between the skull and underlying dura. EEG leads were secured with dental acrylic. An EMG lead was inserted in the neck muscle. The animals were allowed to recover for 24 hrs, then glass electrodes used for ECoG were inserted in the contralateral burr holes to obtain dual recordings of cortical activity, as well as EMG (7-9).

Sleep versus wakefulness was manually scored by visual inspection of the mice behavior every 5 min in radiolabeled clearance studies to avoid contamination of the equipment. Mice in the awake group were kept alert by gentle manipulation of their cages.

### **Iontophoretic tetramethylammonium (TMA) quantification of the interstitial space volume**

All experimental procedures were adapted from the previous studies(10) (11). The single barrel iontophoresis microelectrode (tip diameter of 2-3  $\mu\text{m}$ ) contained 150 mM TMA-chloride and 10  $\mu\text{M}$  Alexa 488. A series of currents of 20 nA, 40 nA and 80 nA were applied by a dual-channel microelectrode preamplifier. For measurements of TMA, microelectrodes with an outer diameter of 2–3  $\mu\text{m}$  were fabricated from double-barreled theta-glass using a tetraphenylborate-based ion exchanger. The TMA barrel was backfilled with 150 mM TMA-chloride, whereas the reference barrel contained 150 mM NaCl and 10  $\mu\text{M}$  Alexa 568. All recordings were obtained by inserting the two electrodes to a depth of 150  $\mu\text{m}$  below the cortical surface. Recording electrodes were inserted 2.5 mm lateral and 2 mm posterior to bregma or in the same location as the CSF tracer imaging analysis. The electrode tips were imaged after insertion using 2-photon excitation to determine the exact distance between the

electrodes (typically  $\sim 150 \mu\text{m}$ ). The TMA signal was calculated by subtracting the voltage measured by the reference barrel from the voltage measured by the ion-detecting barrel using a dual-channel microelectrode preamplifier. The Nikolsky equation was used for calibration of the TMA electrodes based on measurements obtained in electrodes containing 0.5, 1, 2, 4, and 8 mM TMA-chloride in 150 mM NaCl. The TMA measurements were acquired relative to similar recordings obtained in 0.3% agarose prepared from a solution containing 0.5 mM TMA and 150 mM NaCl. A custom-made MatLab software, 'Walter', developed by C. Nicholson was used to calculate  $\alpha$  and  $\lambda$  values (10). The mixture of norepinephrine receptor antagonists (prazosin, atipamezole and propranolol, all at 25  $\mu\text{M}$ ) (2) were dissolved in aCSF and applied at the surface of the brain in the experiments involving recordings of interstitial space using TMA microelectrodes. Due to the small volume administered of CSF administered in cisterna magna, higher concentrations of the NE receptor antagonists (2 mM) were used in experiments involving CSF tracer imaging.

### **Microdialysis and norepinephrine analysis of dialysate**

To evaluate the norepinephrine level in mouse brain under different conditions, a dialysis guide cannula was positioned within cortex, the location of the cannula tip was AP + 2.0, ML + 0.3 from bregma and DV -1.0 from dura. The guide cannula was secured to the skull with dental cement. After implantation, animals were allowed to recover for at least 24 hours and were then training for head restraint as described above. Dialysis probe was inserted into the cannula and perfused with filtered aCSF (145 mM NaCl, 2.7 mM KCl 1.2 mM  $\text{CaCl}_2$  2mM  $\text{Na}_2\text{HPO}_4$  and 1.0 mM  $\text{MgCl}_2$ , adjusted to pH 7.4) at a rate of 0.33  $\mu\text{l}/\text{min}$  for 12 hours. On test day, dialysate samples were obtained from mice at 1 hr intervals while either freely moving in their cage (unrestrained), restrained, followed by another 1 hr period of free movement in their cage (unrestrained). Finally, the animals were anesthetized with ketamine/xylazine and the last 1 hr microdialysis sample collected. The 20  $\mu\text{l}$  dialysates were immediately analyzed by HPLC-EC system consisting of an ESA 584 pump, an ESA MD-160, 1.5x250 mm, 5  $\mu\text{M}$  column, and an ESA 5600A Coulochem II detector with an ESA 5041 analytical cell( + 220v). The mobile phase consisted of 150 mM ammonium acetate, 140  $\mu\text{M}$  EDTA, 15% methanol (vol/vol), and 5%

Acetonitrile with a pH of 6.0, which was filtered and degassed prior to use. The flow rate through the system was 0.15 ml/min.

### **Radiolabeled tracer influx and clearance**

To evaluate the absolute proportion of subarachnoid CSF that enters the brain, radio-labeled  $^3\text{H}$ -mannitol (0.1  $\mu\text{Ci}$ ) was delivered intracisternally. After 15, 30 or 45 min, animals were rapidly decapitated, the skull opened, the dura removed and the brain harvested. The brain was solubilized in 2 ml Soluene at 45°C overnight. 10 ml Hionic Fluor liquid scintillation cocktail was added and radioactivity was measured in a Multipurpose Scintillation Counter. Brain radioactivity was normalized to total radioactivity detected in a 10  $\mu\text{l}$  aliquot transferred directly into a scintillation vial immediately before intracisternal radio-tracer injection and expressed as the % of total injected radioactivity.  $^3\text{H}$ -mannitol accumulation in the brain was compared by 2-way ANOVA with Bonferroni's post-hoc test.

To evaluate the rates of interstitial fluid and solute clearance from the brain, radio-labeled tracers ( $^{125}\text{I}$ -A $\beta_{1-40}$  and  $^{14}\text{C}$ -inulin) were injected stereotactically into the brain parenchyma. Radio-iodinated A $\beta$  was used since there was no significant difference between the clearances of A $\beta$  from brain using radio-iodinated A $\beta$  or non-radio labeled A $\beta$  (ELISA) (12). Briefly, a stainless steel guide cannula was implanted into the right frontal cortex of anesthetized 10-12 weeks old male mice (2% isoflurane) with the coordinates of the cannula tip at 0.7 mm anterior and 3.0 mm lateral to the bregma, and 1.3 mm below the surface of the brain. Animals were allowed to recover after surgery and the experiments performed 12-24 hrs after the guide tube cannulation, as reported previously (13, 14). Clearance of A $\beta$  and inulin were studied under three conditions: anesthetic (100 mg/kg ketamine and 10 mg/kg xylazine) (23 mice), awake (25 mice) and sleeping (29 mice). In each mouse, a small volume of mock CSF (0.5  $\mu\text{L}$ ), containing  $^{125}\text{I}$ -labeled A $\beta$  (10 nM monomer  $^{125}\text{I}$ -A $\beta_{1-40}$ ) and tracer levels of  $^{14}\text{C}$ -inulin (0.05  $\mu\text{Ci}$ ), was simultaneously injected (33 GA cannula) into brain ISF over 5 minutes. At the end of the experiments (predetermined time-points between 10 and 240 min) the brain was removed and prepared for radioactivity analysis and TCA analyses of A $\beta$  (14). Studies with  $^{125}\text{I}$ -labeled A $\beta$  have demonstrated that radiolabeled A $\beta$  remains mainly intact in brain ISF (> 95%) within 300

min of *in vivo* clearance studies (15).  $^{125}\text{I}$  radio-activities were determined using a gamma counter. For  $^{14}\text{C}$  counting, the samples were solubilized in 0.5 ml tissue solubilizer overnight, followed by addition of 5 ml of scintillation cocktail and analyzed in a liquid scintillation counter.

*Calculations of clearance rates:* The percentage of radioactivity remaining in the brain after microinjection was determined as % recovery in brain =  $100 \times (N_b/N_i)$  (eq. 1), where,  $N_b$  is the radioactivity remaining in the brain at the end of the experiment and  $N_i$  is the radioactivity injected into the brain ISF, i.e., the d.p.m. for  $^{14}\text{C}$ -inulin and the c.p.m. for the TCA-precipitable  $^{125}\text{I}$ -radioactivity. Inulin was used as a metabolically inert polar molecule which is neither transported across the BBB nor retained by the brain; its clearance rate provides a measure of the ISF bulk flow and was calculated as  $N_B(\text{inulin})/N_i(\text{inulin}) = \exp(-k_{\text{inulin}} * t)$  (eq. 2). The total clearance of  $\text{A}\beta_{40}$  was determined using a similar equation. Rate constants and half-time ( $t_{1/2}$ ) were determined using Prism version 3. Clearance data were analyzed using 2-way ANOVA and Bonferroni's post-hoc test to determine differences at individual time points.

## Supplementary Figures

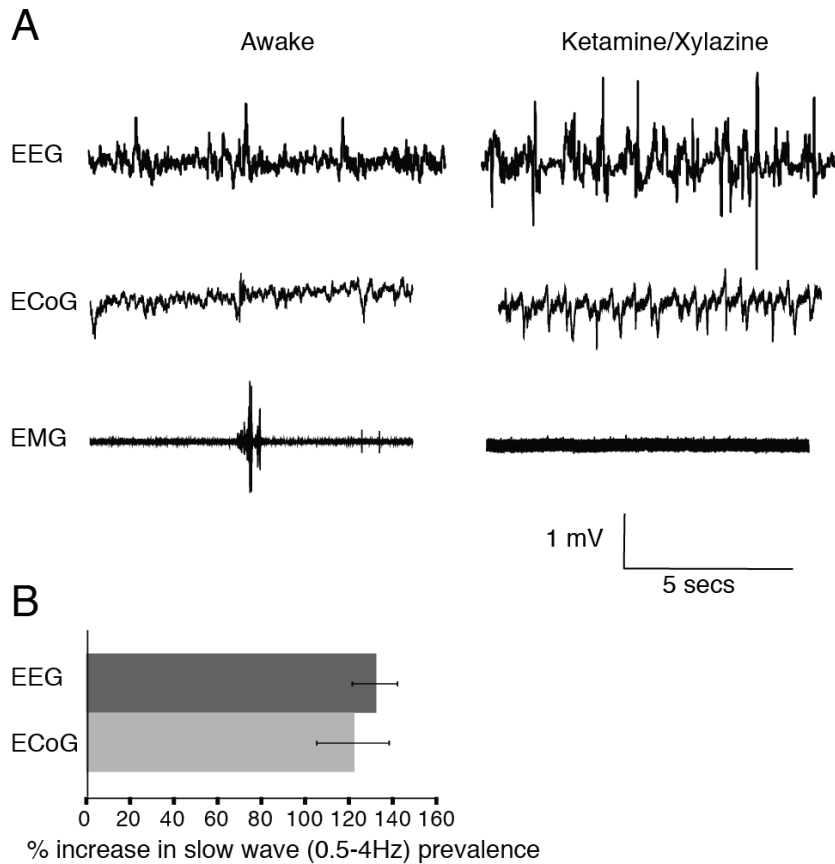


**Fig. S1. Validation of Sleep/Wake Scoring**

Standard EEG electrodes are fairly large (1-2 mm) and rest on top of the dura. To avoid interference with CSF convective fluxes in the subarachnoid space due to placement of EEG electrodes, ECoG was recorded in combination with EMG in all in vivo 2-photon imaging experiments. To evaluate how accurately ECoG/EMG recordings detect transitions in the arousal state, standard EEG recordings were compared to cortical ECoG recordings obtained in the same animals. **(A)** Standard EEG electrodes were positioned over the left hemisphere (2.5 mm lateral and 2 mm posterior to bregma) the day before the experiments. ECoG recordings were collected by inserting a glass micropipette 150  $\mu$ m below the pial surface in the right hemisphere (2.5 mm lateral and 2 mm posterior to bregma). The EMG electrode was inserted in the neck muscles. **(B)** Comparison of percentage increase in slow wave prevalence upon transition from awake to ketamine/xylazine anesthesia using standard EEG electrodes and ECoG recordings (n = 5).

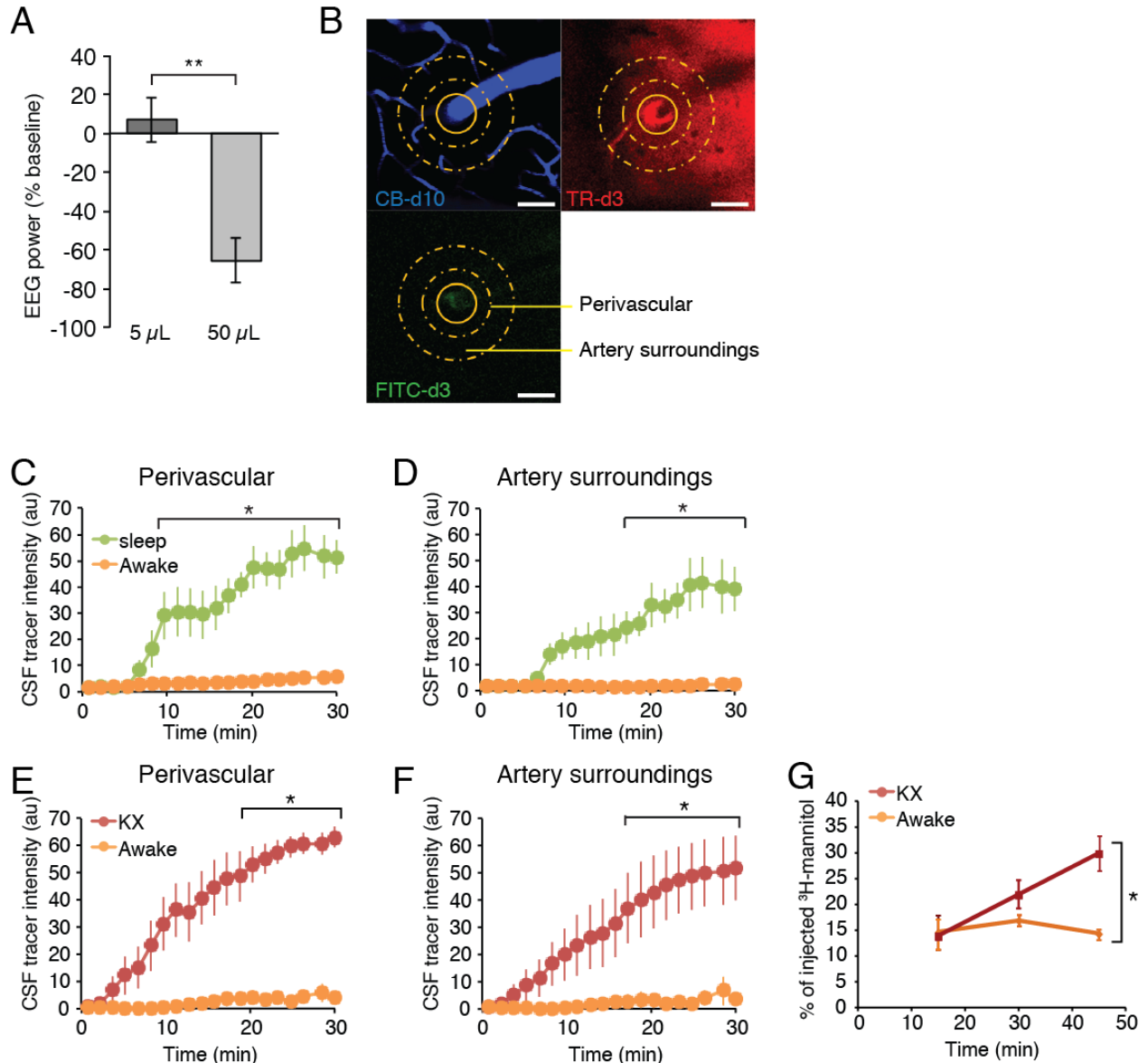


**Fig. S2. Effect of intracisternal injection on ECoG and comparison of perivascular and parenchymal CSF tracer influx in two different arousal states in the same animal.**

**(A)** Analysis of the effect of intracisternal injection of artificial cerebrospinal fluid on (aCSF) ECoG power. The aCSF contained TR-d3 and FITC-d3 (both 5%) and was injected at a rate of 1  $\mu\text{l}/\text{min}$ . Injecting 5  $\mu\text{l}$  was not associated with changes in ECoG power, whereas the 50  $\mu\text{l}$  injections triggered a transient dampening of ECoG signal amplitude (\* $P < 0.05$  One-Way ANOVA with Tukey Post hoc test). **(B)** To establish the effect of the arousal state on CSF tracer influx kinetics, Texas red or FITC labeled dextran with identical molecular weight (3kD) were injected in cisterna magna in the same animal during two different arousal states. We

compared the influx of Texas red (TR-d3) and FITC (FITC-d3) dextran in sleeping mice and then again after waking them up by gentle movement of their tail. These experiments were done when mice are naturally asleep (12-2pm). In another group of mice, tracer influx in awake mice was compared to tracer influx after the mice were anesthetized with ketamine/xylazine. These experiments were performed when mice were naturally awake (8-10pm). Tracer influx was analyzed along peri-arterial pathways and in the cortical parenchyma using in vivo 2-photon laser scanning microscopy through a closed cranial window. The cerebral vasculature was visualized via intravenous injection of Cascade Blue-dextran-10 (CB-d10) and penetrating arterioles were identified by morphology and the flow pattern: surface arteries passed superficially to surface veins and exhibited less branching at superficial cortical depths. The Image analysis of intracisternal tracer penetration was conducted with ImageJ software (NIH) with the UCSD plugin set. Imaging planes 100  $\mu\text{m}$  below the cortical surface were selected for the analysis. To define peri-arterial tracer movement, a circular region of interest (ROI, 25 pixels in diameter) was defined surrounding penetrating arteriole (yellow solid circle). To define tracer movement into peri-arterial brain tissue, a donut-shaped ROI was defined that had an external diameter of 150 pixels and an internal diameter of 50 pixels (thus excluding the paravascular ROI, yellow dashed donuts) (3). Both circles were centered around penetrating arterioles. Scale bars: 40  $\mu\text{m}$ . **(C-F)** Mean pixel intensity within these ROIs was measured at each time point in XYZT time-lapse movies collected at 5 min intervals. The CSF tracer moved readily into the cortex along penetrating arterioles and into the brain parenchyma in the sleeping and anesthetized state (green and red lines), but not in awake mice (orange line; \* $p < 0.05$ ,  $n = 6$  each group). **(G)** Radio labeled  $^3\text{H}$ -mannitol was injected intracisternally in awake and anesthetized mice. Brains were harvested 15, 30 or 45 min after radio-tracer injection to quantify radiotracer accumulation within the brain parenchyma. Brains were solubilized in Soluene, and total brain count was detected by liquid scintillation counting. Total  $^3\text{H}$  counts from brain divided by total injected  $^3\text{H}$ -mannitol were used to calculate CSF influx (3).  $^3\text{H}$ -mannitol accumulated gradually in brain with time in mice anesthetized with ketamine/xylazine, but not significantly in awake mice (\* $p < 0.05$ ,  $n = 4-6$  each group, 2-way ANOVA with Bonferroni's post-hoc test).

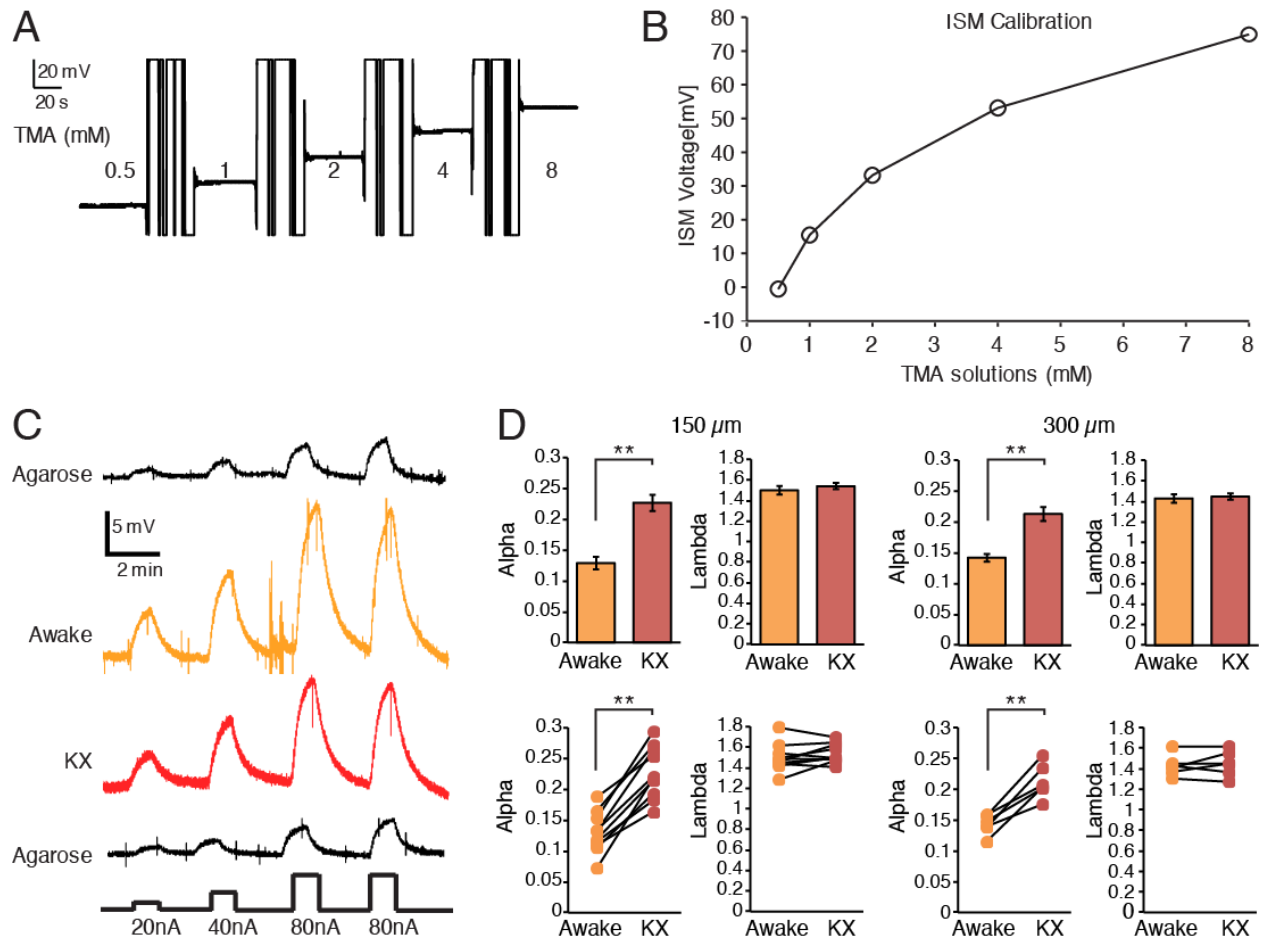


**Fig. S3. Measurement of interstitial space volume fraction and tortuosity using the iontophoretic TMA<sup>+</sup> method**

**(A)** TMA-ion selective microelectrodes (ISMs) were calibrated in aCSF solution containing 0.5, 1, 2, 4, and 8 mM TMA-chloride. **(B)** The voltage *versus* the TMA<sup>+</sup> concentration was plotted and fitted to Nikolsky equation (16). **(C)** Representative examples of TMA<sup>+</sup> diffusion curves from one experiment in which recordings were first obtained in 1) agarose, 2) awake mouse (150  $\mu\text{m}$  below the cortical surface), 3) same mouse after administration of ketamine/Xylazine (without moving the electrodes), and 4) agarose. Four current injections (20, 40, 80, and 80 nA) were analyzed. **(D)** Alpha and lambda collected at a depth of 150 *versus* 300  $\mu\text{m}$  below the cortical surface did not differ significantly in either the awake or the ketamine/xylazine anesthetized state ( $n = 10$  for 150  $\mu\text{m}$ ,  $n = 6$  for 300  $\mu\text{m}$ ; \*\*  $p < 0.01$ , paired t test).

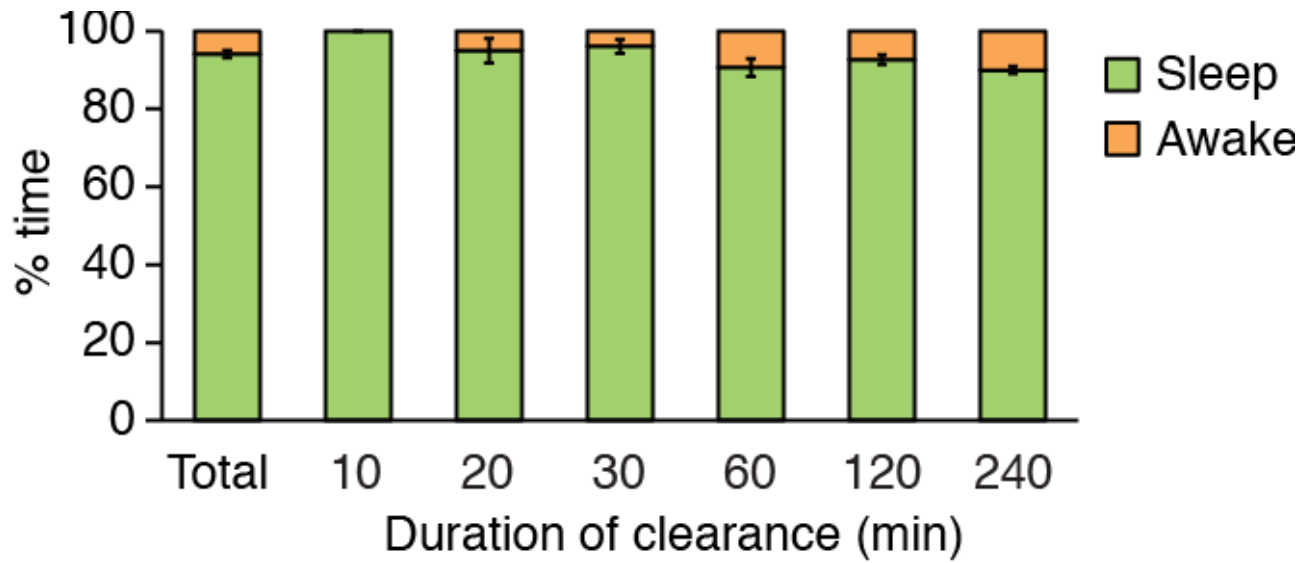


**Fig. S4. Sleep scoring for clearance studies**

Recordings of ECoG and EMG were not obtained in radiolabeled clearance studies to avoid contaminating the equipment. Instead animals in the awake group were kept alert during the experiments by gentle movement of their cages. Clearance data for sleep was obtained by keeping the room quiet, while an immobilized observer scored the activity state of the mice (sleep versus awake) every 5 min throughout the experiments. The relative amount of sleep in the sleep group during clearance was calculated and plotted. None of the animals in the ketamine/xylazine woke up during the clearance phase ( $n = 4-27$ ,  $P = 0.06$ , one way ANOVA.)

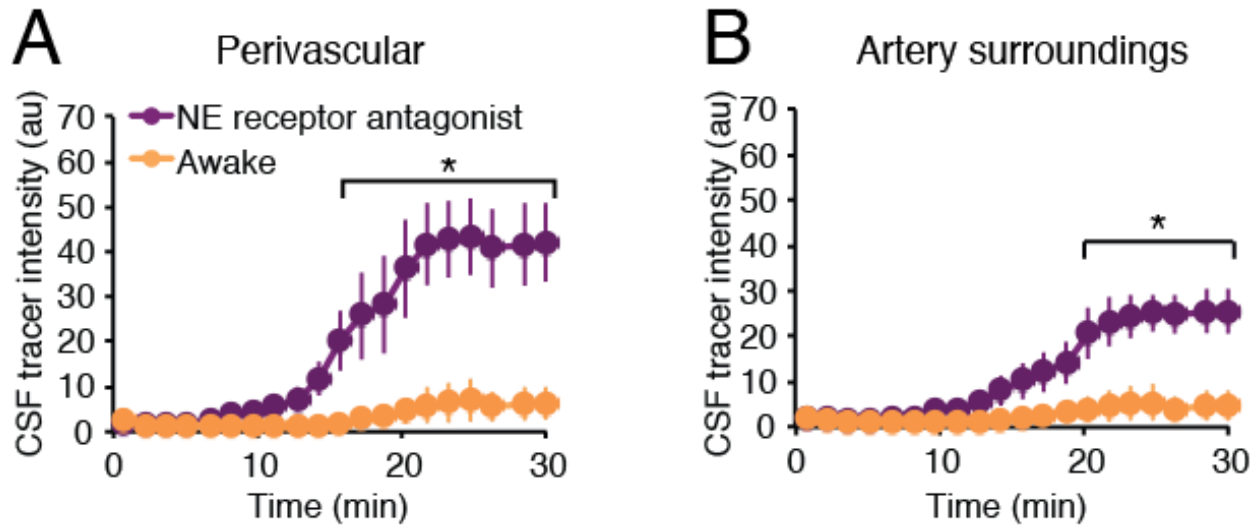


**Fig. S5. Intracisternal administration of a mixture of norepinephrine receptor antagonists increases CSF tracer influx.**

A mixture of norepinephrine receptor antagonists (prazosin, atipamezole and propranolol, each 2 mM), was injected into the cisterna magna of awake mice starting with a bolus of 5  $\mu$ l (1 $\mu$ l/min) followed by a constant infusion of 0.167 $\mu$ l/min with a syringe pump until the end of experiment. Using the same approach to detect influx of CSF tracers shown in Fig. S2, the kinetics of tracer influx were compared before and 15 min after NE receptor antagonist administration. Influx of the two dextrans of same molecular weight (TR-d3 and FITC-d3) injected in awake mice orange line prior to administration of norepinephrine receptor antagonists and again 15 min after the injection of the norepinephrine receptor antagonists (purple line) were calculated along peri-arterial pathways and in the cortical parenchyma (\* $p < 0.05$ ,  $n = 6$  each group, two-way ANOVA with Bonferroni test).

## References and Notes

1. X. Wang *et al.*, Astrocytic Ca<sup>2+</sup> signaling evoked by sensory stimulation in vivo. *Nature neuroscience* **9**, 816 (Jun, 2006).
2. C. M. Constantinople, R. M. Bruno, Effects and mechanisms of wakefulness on local cortical networks. *Neuron* **69**, 1061 (Mar 24, 2011).
3. J. J. Iliff *et al.*, A Paravascular Pathway Facilitates CSF Flow Through the Brain Parenchyma and the Clearance of Interstitial Solutes, Including Amyloid beta. *Sci Transl Med* **4**, 147ra111 (Aug 15, 2012).
4. G. F. Tian *et al.*, An astrocytic basis of epilepsy. *Nature medicine* **11**, 973 (Sep, 2005).
5. N. A. Oberheim *et al.*, Loss of astrocytic domain organization in the epileptic brain. *The Journal of neuroscience : the official journal of the Society for Neuroscience* **28**, 3264 (Mar 26, 2008).
6. A. S. Thrane *et al.*, General anesthesia selectively disrupts astrocyte calcium signaling in the awake mouse cortex. *Proceedings of the National Academy of Sciences of the United States of America* **109**, 18974 (Nov 13, 2012).
7. E. N. Bruce, M. C. Bruce, S. Vennelaganti, Sample entropy tracks changes in electroencephalogram power spectrum with sleep state and aging. *J Clin Neurophysiol* **26**, 257 (Aug, 2009).
8. K. Hellman, P. Hernandez, A. Park, T. Abel, Genetic evidence for a role for protein kinase A in the maintenance of sleep and thalamocortical oscillations. *Sleep* **33**, 19 (Jan, 2010).
9. H. W. Steenland, V. Wu, H. Fukushima, S. Kida, M. Zhuo, CaMKIV over-expression boosts cortical 4-7 Hz oscillations during learning and 1-4 Hz delta oscillations during sleep. *Mol Brain* **3**, 16 (2010).
10. C. Nicholson, Ion-selective microelectrodes and diffusion measurements as tools to explore the brain cell microenvironment. *Journal of neuroscience methods* **48**, 199 (Jul, 1993).

11. C. Nicholson, Quantitative analysis of extracellular space using the method of TMA<sup>+</sup> iontophoresis and the issue of TMA<sup>+</sup> uptake. *Can J Physiol Pharmacol* **70 Suppl**, S314 (1992).
12. R. D. Bell *et al.*, Transport pathways for clearance of human Alzheimer's amyloid beta-peptide and apolipoproteins E and J in the mouse central nervous system. *J Cereb Blood Flow Metab* **27**, 909 (May, 2007).
13. J. R. Cirrito *et al.*, P-glycoprotein deficiency at the blood-brain barrier increases amyloid-beta deposition in an Alzheimer disease mouse model. *J Clin Invest* **115**, 3285 (Nov, 2005).
14. R. Deane *et al.*, LRP/amyloid beta-peptide interaction mediates differential brain efflux of Abeta isoforms. *Neuron* **43**, 333 (Aug 5, 2004).
15. R. Deane, A. Sagare, B. V. Zlokovic, The role of the cell surface LRP and soluble LRP in blood-brain barrier Abeta clearance in Alzheimer's disease. *Curr Pharm Des* **14**, 1601 (2008).
16. C. Nicholson, P. Kamali-Zare, L. Tao, Brain Extracellular Space as a Diffusion Barrier. *Computing And Visualization In Science* **14**, 309 (Oct 1, 2011).